

Molecular Dynamics and Free Energy Studies on the Wild-Type and Mutated HIV-1 Protease Complexed with Four Approved Drugs: Mechanism of Binding and Drug Resistance

Stefano Alcaro,^{*,†} Anna Artese,[†] Francesca Ceccherini-Silberstein,[‡] Francesco Ortuso,[†] Carlo Federico Perno,[‡] Tobias Sing,[§] and Valentina Slicher[‡]

Laboratorio di Chimica Farmaceutica Computazionale - Dipartimento di Scienze Farmacobiologiche, Università “Magna Gracia” di Catanzaro, Campus Universitario, Viale Europa, 88100 Catanzaro, Italy, Dipartimento di Medicina Sperimentale e Biochimica, Università “Tor Vergata”, Via Montpellier, 1, 00133, Roma, Italy, and Max-Planck-Institute for Informatics, Saarbrücken, Germany

Received January 13, 2009

The current strategy to improve the quality of life of Human Immunodeficiency Virus (HIV) infected individuals through suppressing viral replication and maintaining the virus at low to undetectable levels is based on highly active antiretroviral therapy (HAART). Protease inhibitors are essential components of most HAART protocols and are often used as the first line of treatment. However, a considerable percentage of new HIV-1 infections are caused by viruses carrying antiretroviral drug-resistant mutations. In this paper molecular dynamics, docking simulations, and free energy analysis of mutated HIV protease complexes were used to estimate the influence of different drug resistance-associated mutations in lopinavir, amprenavir, saquinavir, and atazanavir protease recognition. In agreement with virological and clinical data, the structural analysis showed that the single mutations V82A, I84V, and M46I are associated with higher energetic values for all analyzed complexes with respect to wild-type, indicating their decreased stability. Interestingly, in atazanavir complexes, in the presence of the L76V substitution, the drug revealed a more productive binding affinity, in agreement with hypersusceptibility data.

INTRODUCTION

The human immunodeficiency virus type I aspartic protease (HIV-1 protease) cleaves the gag and pol nonfunctional polypeptide into functional proteins essential for the maturation of infectious HIV particles.

For its crucial role in the HIV-1 life cycle, protease (PR) represents an important target for antiretroviral therapy.¹

The initial knowledge of the structures of retroviral proteases came from the crystallographic studies carried out from RSV (Respiratory Syncytial Virus) and subsequently from HIV-1 in 1989.² These analyses indicated the homodimeric enzyme structure and the active site as very similar to that of the pepsin-like proteases. Thus, the general topology of the two enzymes is similar, with the main difference being that the dimer interface in HIV-1 PR is made up of four short strands, rather than the six long strands present in the pepsins. The N-terminal β -strand described by residues 1–4 forms the outer part of the interface β -sheet. The β -strand created by residues 9–15 continues through a turn into another β -strand, which terminates at the active-site triad (D25-T26-G27). Following the active-site loop is the last β -strand, containing residues 30–35. In the second half of the molecule residues 43–49 form the first β -strand, which belongs to the flap, a β -hairpin that covers the active

Table 1. Z-Score Resistance Data¹³ Calculated for the PR Complexes in the Presence of the Analyzed PIs (**LPV**, **APV**, **SQV**, **ATV**)

PI	Z-score				
	WT	L76V	I84V	V82A	M46I
LPV	0.00	4.04	10.02	N.A.	N.A.
APV	0.00	9.98	N.A.	N.A.	5.79
SQV	0.00	N.A.	10.80	N.A.	2.15
ATV	0.00	−0.30	N.A.	10.56	N.A.

site and participates in the binding of inhibitors and substrates. The other strand in the flap (residues 52–58) forms a part of a long β -chain (residues 52–66). The β -chain described by residues 69–78, after a loop at residues 79–82, continues as another strand (residues 83–85), which leads directly to a well-defined helix (residues 86–94).³

The active-site triad is located in a loop whose structure is stabilized by a network of hydrogen bonds. The carboxylate groups of D25 from both chains are nearly coplanar and show close contacts. The network is quite rigid due to the interaction in which each T26 OG1 accepts a hydrogen bond from the T26 main-chain NH of the opposing loop.⁴

Cocrystals of HIV-1 PR with a variety of inhibitors have been deposited in the Protein Data Bank (PDB)⁵ and are useful to investigate their best poses by molecular modeling techniques. Binding of an inhibitor introduces substantial conformational changes to the enzyme. The overall movement of the subunits can be described as a rotation around a hinge axis located in the subunit β -sheet interface,

* Corresponding author phone: +39 0961, 3694197; fax: +39 0961, 391490; e-mail: alcaro@unicz.it.

[†] Università “Magna Gracia” di Catanzaro.

[‡] Università “Tor Vergata”.

[§] Max-Planck-Institute for Informatics.

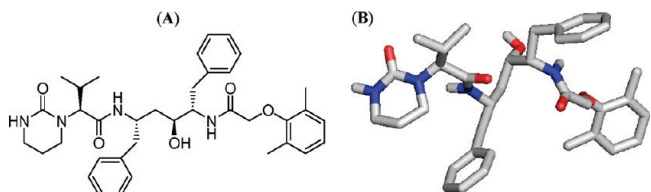


Figure 1. Two-dimensional (A) and three-dimensional (B) structures of LPV obtained using PDB model 1mui.¹⁹

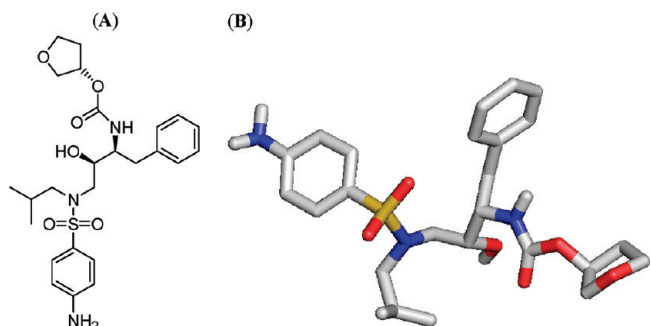


Figure 2. Two-dimensional (A) and three-dimensional (B) structures of APV obtained using PDB model 1T7J.²⁰

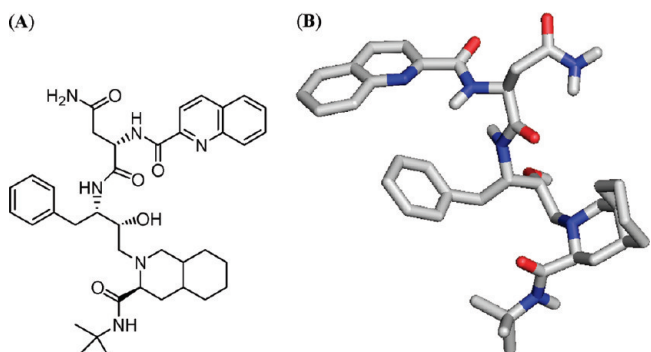


Figure 3. Two-dimensional (A) and three-dimensional (B) structures of SQV obtained using PDB model 2NMW.²¹

accompanied by a very large motion of the flap region.⁶ Most of the inhibitors cocrystallized with HIV-1 PR are bound in the enzyme active site in an extended conformation and make hydrogen bonds mostly with the main-chain atoms of the enzyme. Moreover, the side chains of the inhibitors can be well accommodated in a number of distinct subsites identified in HIV PR, with a preponderance of hydrophobic residues.⁷

To date, ten PR inhibitors (PIs) (indinavir, ritonavir, saquinavir, nelfinavir, amprenavir, lopinavir, atazanavir, tipranavir, fosamprenavir, and darunavir) have been approved by the Food and Drug Administration (FDA) and are clinically available. Unfortunately, when antiretroviral therapy fails to be fully suppressive, viral variants with reduced susceptibilities to PIs can emerge.⁸ Resistance to PIs is mediated by the appearance of PR aminoacid substitutions (at positions either in direct contact with the inhibitor or at

distant sites) that reduce the inhibitor binding affinity to the mutant PR enzyme. These aminoacid substitutions, defined in the literature as major mutations, may deeply impair the PR catalytic activity and, consequently, the replication capacity of the virus. Restoration of the replication capacity is due to the presence of mutations defined in the literature as compensatory mutations.⁹ Several studies have contributed to our current knowledge of the drug-related variants of HIV-1 PR. Mutations at 50 of 99 residues of PR have been related to one or more experimentally tested PIs, thus attesting to the high degree of flexibility of the PR enzyme; 22 of these residues are involved in resistance to the PIs used in clinical practice.¹⁰

Consequently, the elucidation of the molecular recognition of the currently approved PIs in the presence of known mutations responsible to confer resistance is critical for the development of superior inhibitors.

In this manuscript we report a study combining computational analysis of HIV-1 protease crystallographic models and clinical data on drug resistance-associated mutations. Such an analysis, based on the comparison of structural data to resistance profiles, allowed us to understand the influence of some drug resistance-associated mutations in lopinavir, amprenavir, saquinavir, and atazanavir protease recognition. The aim of this work was to create a link between relevant clinically resistance-inducing mutations in HAART patients and the binding properties of HIV-1 PR inhibitors. The medicinal chemist can use this approach to predict the effects of certain HIV-1 PR relevant mutations in the presence of novel inhibitors.

RESULTS AND DISCUSSION

In this study, we have focused the attention to four PI resistance mutations: M46I, V82A, I84V, and L76V. The M46I, V82A, and I84V mutations are known to confer different levels of resistance to the currently available PIs, while the L76V mutation is associated with resistance to lopinavir and darunavir.¹¹

By analyzing a large cohort of HIV-1 infected patients followed in clinical centers from Central Italy, we found that these mutations occurred rarely in drug-naïve patients (M46I: 0.6%, L76V: 0.4%, V82A: 0.5%, and I84V: 0.1%), while their frequency significantly increased ($P < 0.00001$) in patients failing a PI-containing regimen (M46I: 19.6%, L76V: 2.4%, V82A: 16.0%, and I84V: 7.7%). Covariation showed that the M46I established positive and significant ($P < 0.0001$) correlation with either L76V ($\phi=0.22$), or with I84V ($\phi=0.24$), or V82A ($\phi=0.16$). The other mutations were not significantly correlated with each other.

We also analyzed an independent data set of 850 matched genotype-phenotype pairs for each PI, by feature ranking based on support vector regression (SVR), that is a multi-

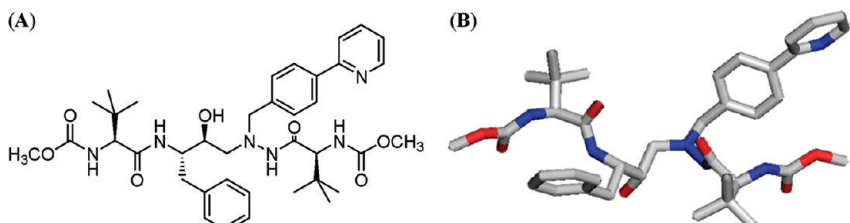


Figure 4. Two-dimensional (A) and three-dimensional (B) structures of ATV obtained using PDB model 2O4K.²²

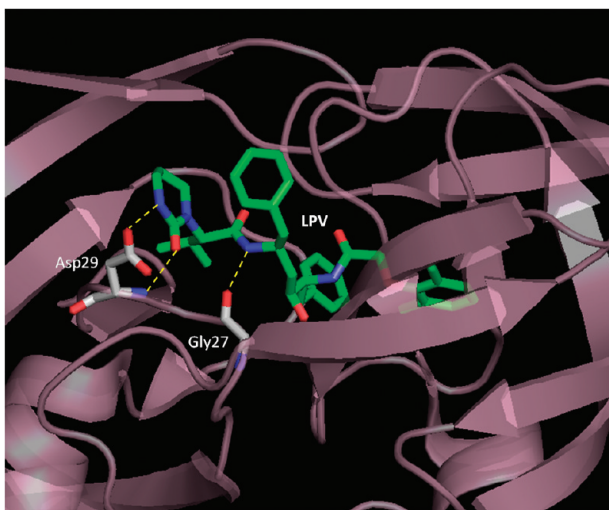


Figure 5. 3D representation of **LPV** interactions in the crystallographic PR complex.¹⁹ The enzyme is shown as a purple cartoon; **LPV** and PR residues in contact are represented, respectively, as green and gray carbon sticks, and the intermolecular hydrogen bonds are indicated as dashed yellow lines.

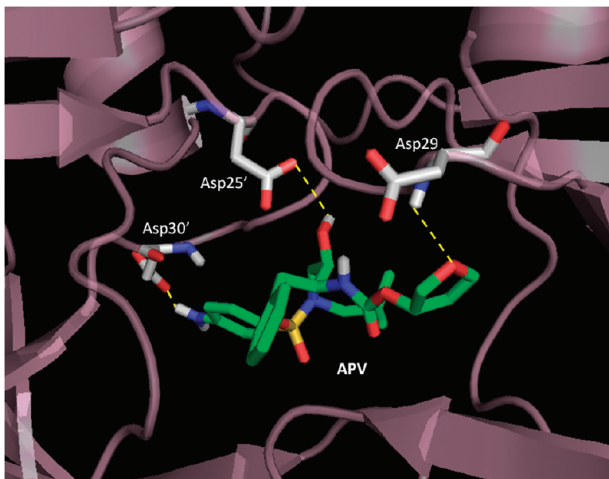


Figure 6. 3D representation of **APV** interactions in the crystallographic PR complex.²⁰ The enzyme is shown as a purple cartoon; **APV** and PR residues in contact are represented, respectively, as green and gray carbon sticks, and the intermolecular hydrogen bonds are indicated as dashed yellow lines.

variate procedure that allows to quantify the impact of mutations relative to other mutations.

In this analysis, we found L76V included among the 25 mutations that directly contribute to resistance to lopinavir. This is consistent with a previous study showing the association of the L76V with lopinavir treatment.¹² In addition, L76V shows a negative score for atazanavir, indicating the association of this mutation with atazanavir hypersusceptibility.

These data are expressed as Z-scores index¹³ (Table 1) and provided us the rationale to evaluate the influence of the selected mutations with respect to lopinavir, amprenavir, saquinavir, and atazanavir PR molecular recognition.

Lopinavir (**LPV**) is a PI developed from ritonavir (Figure 1). Coadministration with low-dose of ritonavir significantly improves the pharmacokinetic properties and hence the activity of **LPV** against HIV-1 PR. Some mutations have been shown to be associated with **LPV** treatment (E34Q, K43T, and K55R) and correlated with

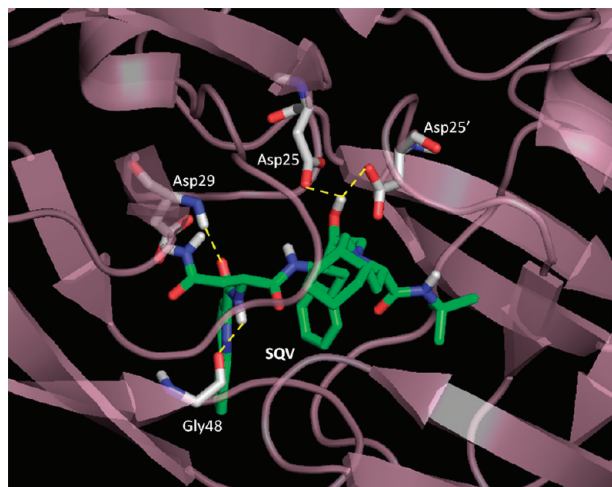


Figure 7. 3D representation of **SQV** interactions in the crystallographic PR complex.²¹ The enzyme is shown as a purple cartoon; **SQV** and PR residues in contact are represented, respectively, as green and gray carbon sticks, and the intermolecular hydrogen bonds are indicated as dashed yellow lines.

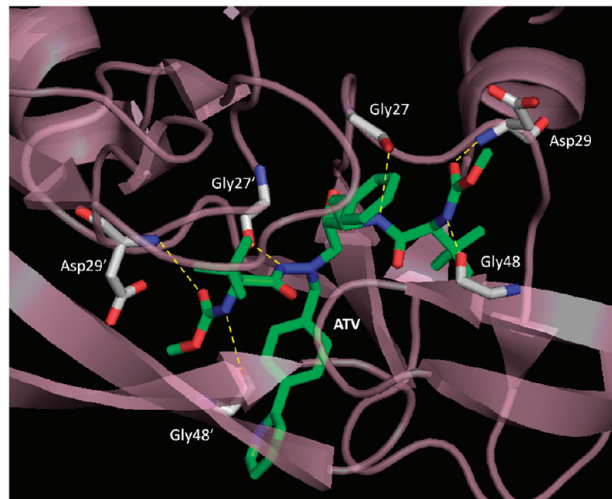


Figure 8. 3D representation of **ATV** interactions in the crystallographic PR complex.²² The enzyme is shown as a purple cartoon; **ATV** and PR residues in contact are represented, respectively, as green and gray carbon sticks, and the intermolecular hydrogen bonds are indicated as dashed yellow lines.

Table 2. Evaluation of the Free Interaction Energy ΔG_{bind}^a Calculated for All PR Studied Complexes in the Presence of the Four Inhibitors **LPV**, **APV**, **SQV**, and **ATV**

PI	ΔG_{bind}^a				
	WT	L76V	I84V	V82A	M46I
LPV	-34.36	-24.96	-31.21	<i>b</i>	<i>b</i>
APV	-39.01	-25.48	<i>b</i>	<i>b</i>	-33.97
SQV	-56.05	<i>b</i>	-31.71	<i>b</i>	-49.46
ATV	-27.77	-33.22	<i>b</i>	-18.52	<i>b</i>

^a Values in kcal/mol were computed by the MM-GBSA approach.²³ ^b Not computed due to the unavailability of Z-score values.

mutations associated with **LPV** resistance (E34Q with either L33F or F53L or K43T with I54A) or clustered with multi-PI resistance mutations (K43T with V82A and I54V or V82A, V32I, and I47V or K55R with V82A, I54V, and M46I).⁸

Table 3. Inhibitor Interacting Residues List of the Analyzed [LPV·PR], [APV·PR], [SQV·PR], and [ATV·PR] Complexes^{a,b}

res ^c	LPV			APV			SQV			ATV		
	WT	I84V	L76V	WT	M46I	L76V	WT	I84V	M46I	WT	V82A	L76V
R8	/	a*	/	/	/	/	a	b*	/	a*	a*b	b*
L23	a	b	/	/	b	ab	/	b	ab	/	a	/
D25	a	*ab	a	a*	a*	*ab	a*	a*	a*b	b*	b*	b*
G27	b*	ab	b*	b	*ab	ab	ab	ab	b	*ab	ab*	*ab
A28	a	ab	ab	b	ab	/	a	a	ab	b	ab	ab
D29	b*	ab*	b*	/	a*	a*	a*b	a*	a*b	b*	/	a*b
D30	a	b	b	/	a*	a	b	/	/	/	/	/
T31	/	b	/	/	/	/	/	/	/	b	/	/
V32	ab	ab	ab	a	a	/	/	a	a	b	a	a
K45	/	/	/	/	/	/	a	/	/	/	/	/
M46	/	/	/	a	/	/	a	/	/	/	/	/
I47	b	b	b	ab	a	a	ab	a	ab	b	b	ab
G48	b	b	b	*ab	*ab	a*	a*	a*	a*	*ab	a*b	a*b
G49	b	b	ab	ab	ab	a	ab	ab	ab	ab	ab	ab
I50	ab*	ab*	ab	a*	*ab	ab*	ab	ab	ab	ab	ab	ab
G51	/	/	/	/	b*	/	/	/	/	/	/	/
G52	/	/	/	/	b*	/	/	/	/	/	/	/
F53	/	/	/	a	/	a	a	a	a	b	b	/
I54	/	/	/	/	/	/	/	/	/	/	/	a
L76	ab	b	/	a	a	a	/	/	/	/	/	/
T80	b	/	b	/	/	/	a*	a	/	/	/	a
P81	a	/	/	b	/	/	ab	/	a	/	ab	/
V82	ab	b	b	/	b	b	ab	b	ab	/	a	/
I84	ab	/	b	/	b	ab	a	a	ab	b	a	a

^a *a* and *b* indicate, respectively, the PR subunits pertinent to the specified residues establishing nonbonded contacts. ^b The asterisks point out hydrogen bonds. ^c The residue is reported as in the WT sequence.

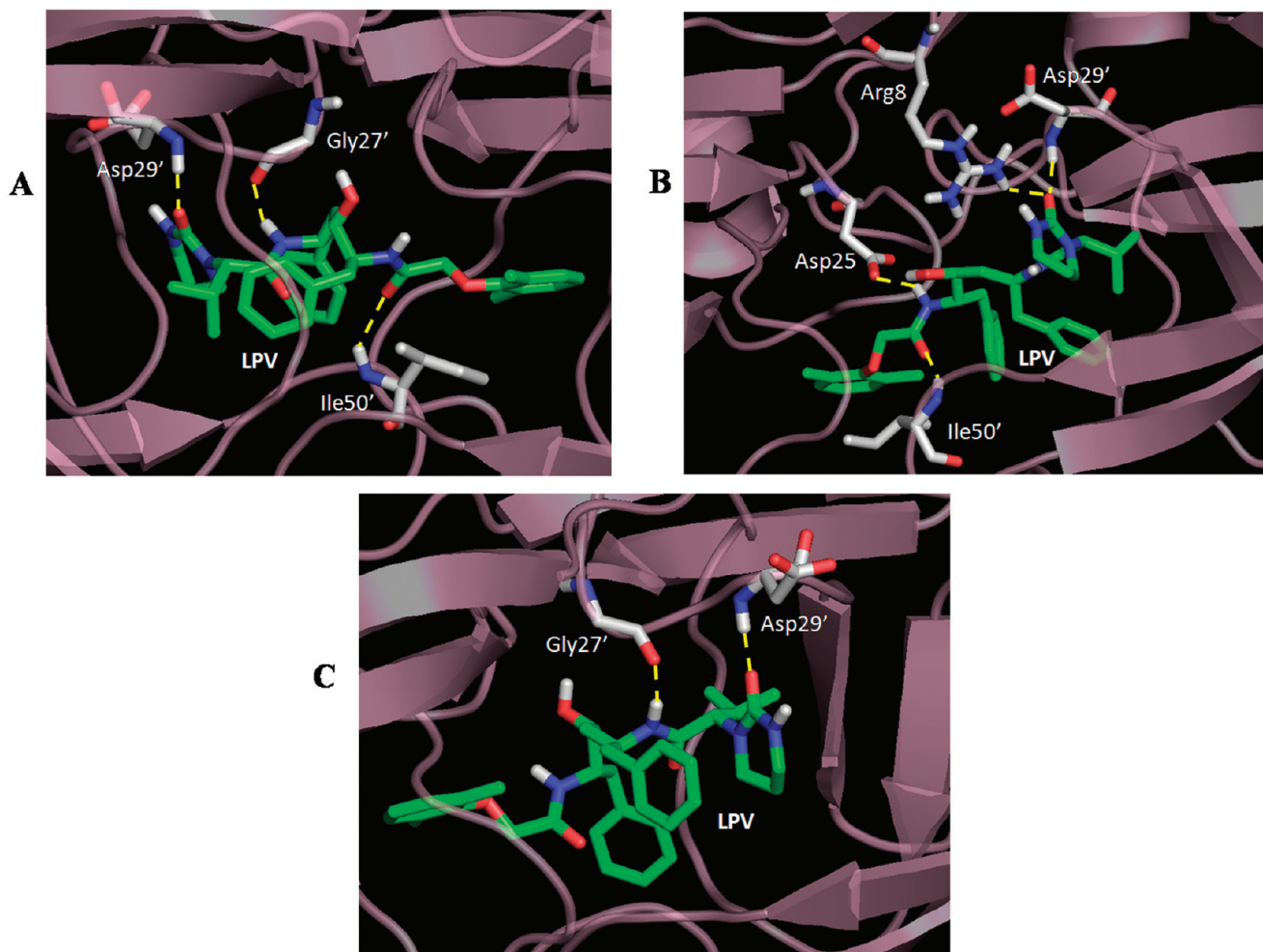


Figure 9. 3D representation of LPV interactions in the obtained most populated (A) wild-type-PR, (B) I84V, and (C) L76V configuration. The enzyme is shown as a purple cartoon; LPV and PR residues in contact are represented, respectively, as green and gray carbon sticks, and the intermolecular hydrogen bonds are indicated as dashed yellow lines.

Amprenavir (**APV**) is a second-generation drug with a hydroxyethylamine sulfonamide scaffold (Figure 2). It was proved to be well tolerated and highly potent in combination

therapies, with a good bioavailability. Although **APV** shows high potency to most drug-resistant variants, significant resistance to it has still been observed when mutations occur

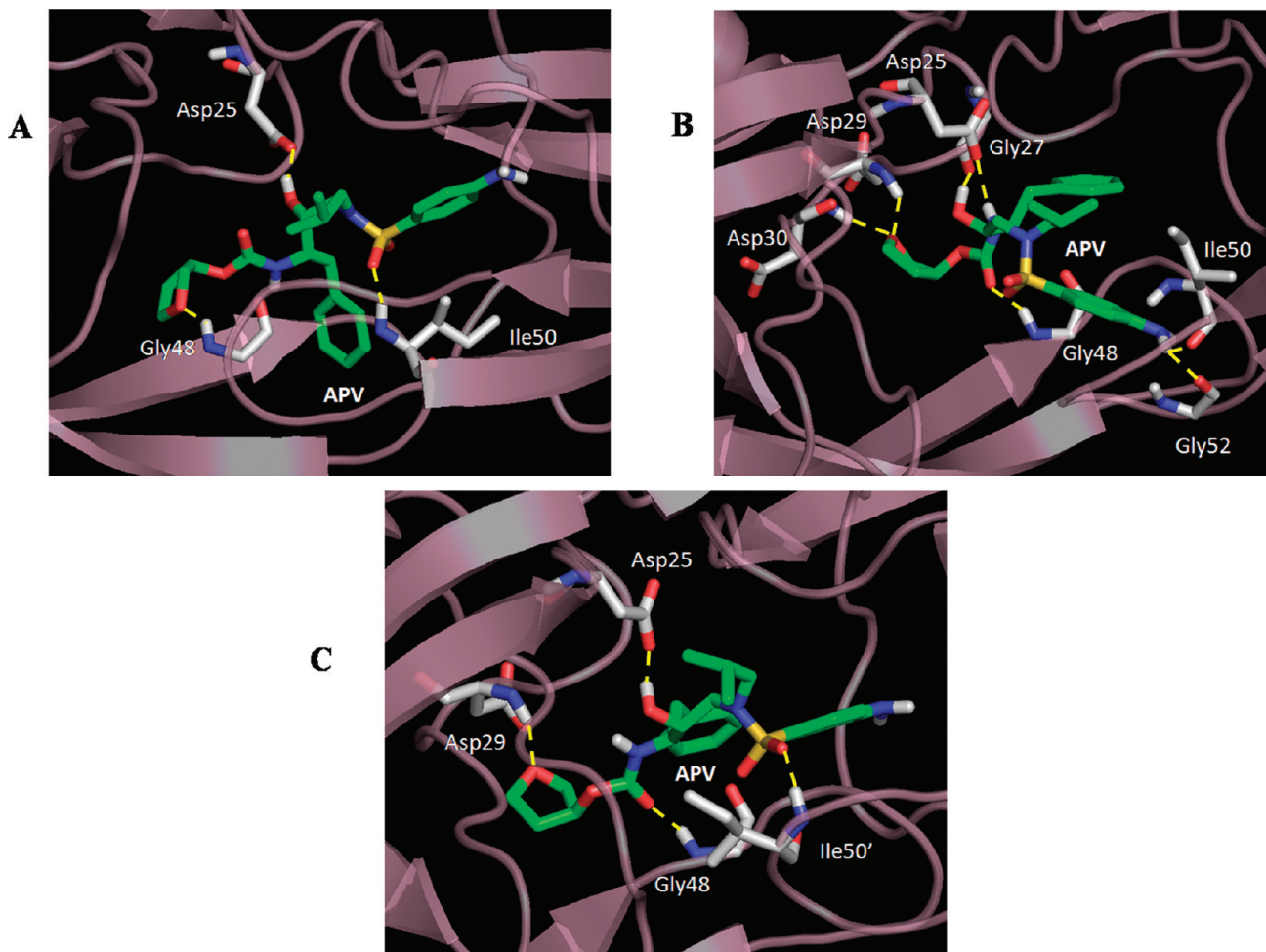


Figure 10. 3D representation of APV interactions in the obtained most populated (A) wild-type-PR, (B) M46I, and (C) L76V configuration. The enzyme is shown as a purple cartoon; APV and PR residues in contact are represented, respectively, as green and gray carbon sticks, and the intermolecular hydrogen bonds are indicated as dashed yellow lines.

at several positions, including the V82/I84 double mutation.¹⁴ The key aminoacid substitution selected during several *in vitro* passage experiments with APV is I50V, located in the active site of the PR and usually accompanied by an M46I/L and, less frequently, by an I47V substitution. Analyzing virus isolates from PI-naïve patients treated with unboosted APV, four resistance pathways involving the substitutions I50V, I54L/M, V32I + I47V and, less commonly, I84V, have been identified and may be accompanied by accessory mutations such as M46I/L or L10I.¹⁵

Saquinavir (SQV) was the first PI to be approved by the FDA in 1995, and it is still widely used in AIDS therapy (Figure 3). SQV was designed to target the wild-type PR, and its chemical structure contains a number of peptidic main chain groups mimicking a natural substrate of PR. Several mutations of I54 are present in isolates with reduced susceptibility to SQV.¹⁶ Moreover a good relationship between genotypic analysis of SQV resistance and data from virus assays confirmed that L90M and G48V are the essential exchanges in the enzyme that determine loss of sensitivity to this inhibitor.¹⁷

Atazanavir (ATV) is a second generation PI reporting for the first time an azapeptide structure (Figure 4). The *in vitro* drug susceptibilities evaluation, carried out onto a large panel of ATV-naïve HIV clinical virus isolates, revealed a distinct resistance profile with respect to other PIs. Viruses isolates

characterization from PI-naïve patients failing ATV therapy highlighted a single I50L mutation of the protease in 100% of ATV resistant isolates.¹⁸

In order to analyze [LPV·PR], [APV·PR], [SQV·PR], and [ATV·PR] complexes, the crystallographic PDB structures with the codes 1MUI¹⁹ (resolution 2.80 Å), 1T7J²⁰ (resolution 2.20 Å), 2NMW²¹ (resolution 1.16 Å), and 2O4K²² (resolution 1.60 Å) were selected, respectively.

Analyzing the crystallographic structures, LPV was found to establish hydrogen bonds to the catalytic G27 and D29 and APV to D25, D29, and D30. Both inhibitors revealed different nonbonded contacts with other PR residues, due to their hydrophobic nature (Figures 5 and 6).

In the crystallographic models, SQV showed hydrogen bonds to D25, D29, and G48 and ATV to the catalytic G27 and D29 and to G48 in both chains. Either the peptidic or the azapeptide inhibitor highlighted several productive nonbonded interactions due to the presence of aromatic rings, as reported in Figures 7 and 8.

With the aim to investigate the influence of the analyzed mutations onto the enzyme conformational properties, we submitted all the studied complexes to molecular dynamics (MD) simulations and Monte Carlo (MC) *in situ* calculations. The obtained conformations were evaluated in terms of interaction free energy expressed as ΔG_{bind} ,²³ as reported in Table 2.

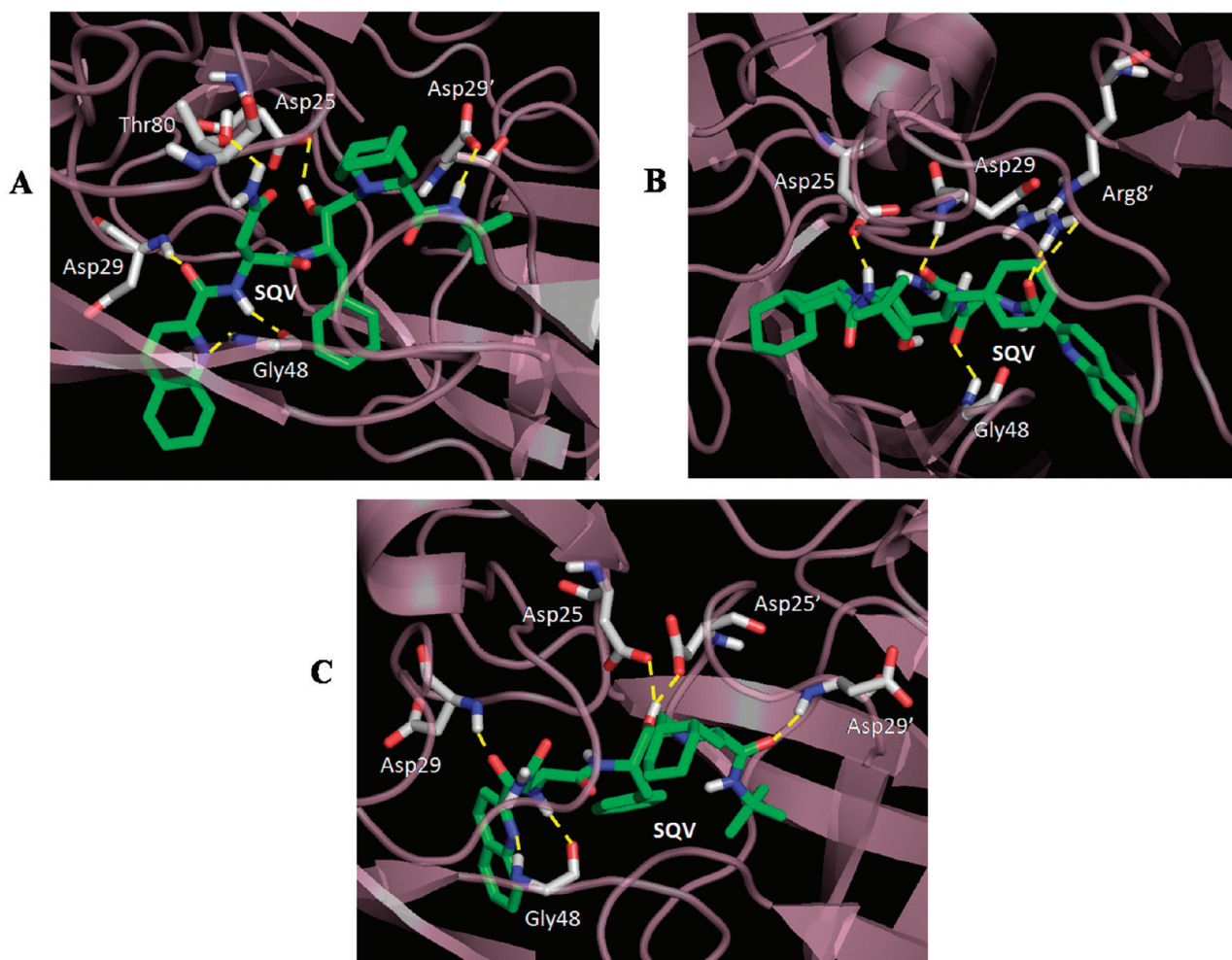


Figure 11. 3D representation of SQV interactions in the obtained most populated (A) wild-type-PR, (B) M46I, and (C) I84V configuration. The enzyme is shown as a purple cartoon; SQV and PR residues in contact are represented, respectively, as green and gray carbon sticks, and the intermolecular hydrogen bonds are indicated as dashed yellow lines.

Such an analysis revealed that in [LPV·PR] complexes I84V and L76V mutated enzymes were associated with an unfavorable energetic profile with respect to WT, indicating their decreased stability.

Considering [APV·PR] complexes, the drug resulted in being less stabilized within the M46I and L76V mutated enzyme versus the WT.

In [SQV·PR] complexes, I84V mutant indicated poor affinity and stability, according to its high resistance index (Table 1), while M46I showed a profile quite similar to WT.

Analyzing ATV complexes, the V82A mutation showed a reduced binding affinity with respect to the WT sequence. Interestingly, in the presence of the L76V substitution, ATV revealed a more stabilized configuration, in agreement with hypersusceptibility data, as indicated by the negative Z-score value (Table 1).

With the purpose to examine the obtained theoretical complexes for the analyzed PR inhibitors, the interactions established between the studied PI within the enzyme active site were evaluated for either wild type (WT) or mutated enzymes (Table 3).

According to the Boltzmann population at room temperature, for the best WT configuration of [LPV·PR] complex several nonbonded contacts and three hydrogen bonds were observed, as shown in Figure 9A. In the most populated [LPV·PR] configuration with the I84V mutation, several

nonbonded contacts and four hydrogen bonds were identified. The accommodation of LPV was well stabilized through an interaction with R8, found to be essential in the PR catalytic site.²⁴ Nonetheless the drug, with respect to the LPV-WT protease complex, lost the crucial hydrogen bond to G27 and some pivotal van der Waals contacts with aminoacids located into the active site, with the drop of its binding affinity (Figure 9B). Examining the most stable LPV-protease complex with the L76V mutation, a lower number of nonbonded interactions was observed if compared to LPV-WT PR complex. Moreover, such a mutation caused a reduced hydrogen bond network and destabilized the [drug·PR] recognition (Figure 9C).

In the WT [APV·PR] global minimum, three hydrogen bonds and several van der Waals interactions were detected (Figure 10A). In particular the sulfonamide inhibitor indicated a hydrogen bond with G48, found to be crucial in substrate binding.²⁵ Examining the interactions of the most stable [APV·PR] complex in the presence of the M46I mutation, an increased hydrogen bond network with respect to the WT complex was observed (Figure 10B). However the drug showed a reduced binding affinity with respect to the WT because of the loss of van der Waals contacts with the aromatic residue F53, resulting in essential hydrophobic interactions with the drug.²⁶

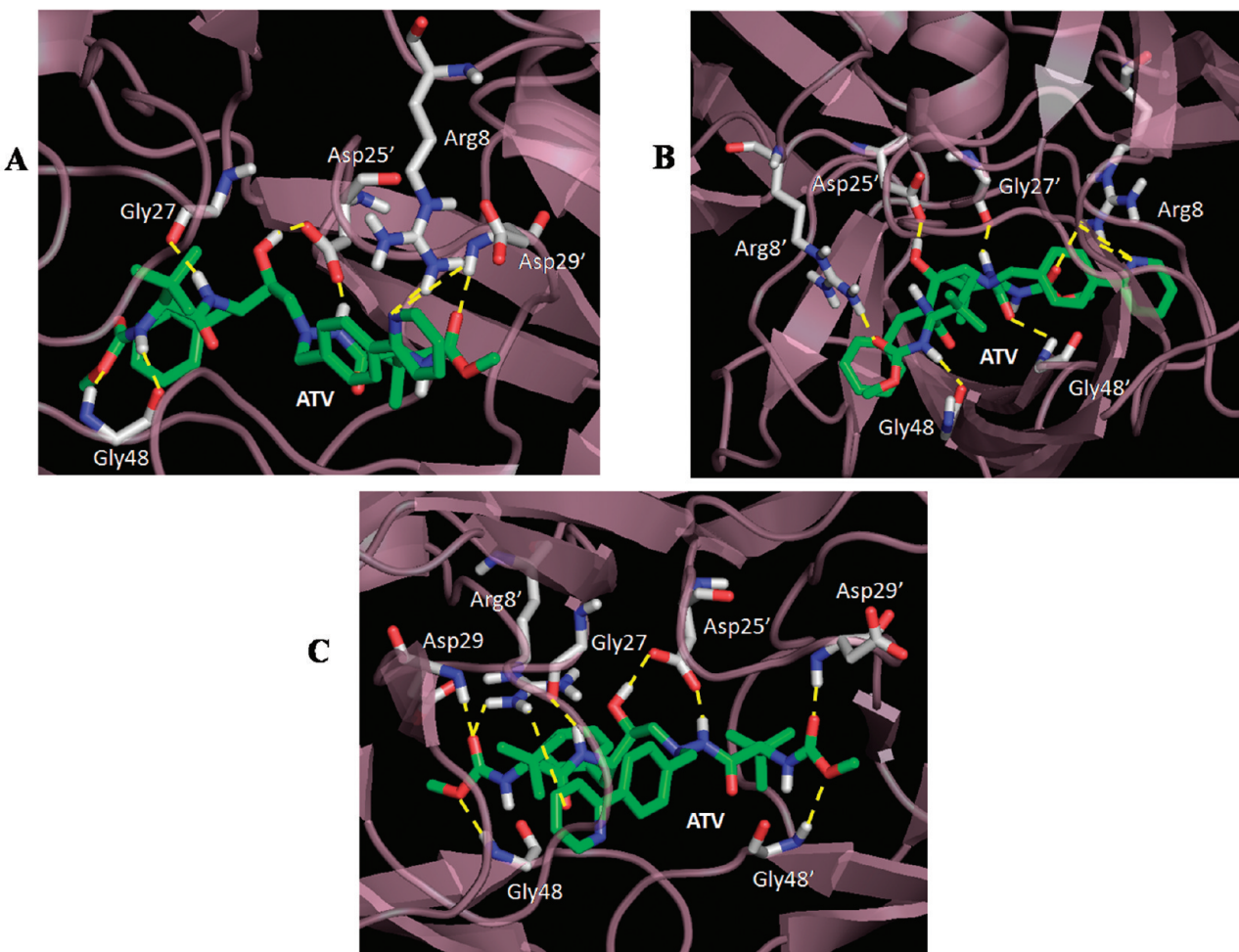


Figure 12. 3D representation of ATV interactions in the obtained most populated (A) wild-type-PR, (B) V82A, and (C) L76V configuration. The enzyme is shown as a purple cartoon; ATV and PR residues in contact are represented, respectively, as green and gray carbon sticks, and the intermolecular hydrogen bonds are indicated as dashed yellow lines.

Considering the most probable configuration of the analyzed complex in the presence of the L76V substitution, APV was found to establish four hydrogen bonds and numerous nonbonded contacts (Figure 10C). Even so, the drug resulted in being poorly stabilized in the PR active site due to a lower number of nonbonded contacts to F53, if compared to the WT sequence.

In the most probable WT [SQV·PR] configuration, the peptidomimetic ligand was well stabilized in the enzyme active site through a large number of nonbonded contacts and six hydrogen bonds with D25, D29 of both chains, G48 and T80 (Figure 11A). Analyzing the most stable configuration in the presence of the M46I substitution, the same hydrogen bond network and a reduced number of van der Waals interactions were observed (Figure 11B). In particular, SQV missed a crucial interaction with R8,²⁷ decreasing its binding affinity. The I84V destabilizing effect of [SQV·PR] complex was associated with the loss of two crucial hydrogen bonds with D29' and T80 and to a lower number of nonbonded contacts with respect to the WT sequence (Figure 11C).

In the WT [ATV·PR] global minimum energy structure, the interactions analysis highlighted several nonbonded contacts and eight hydrogen bonds, as reported in Figure 12A. A high stabilization of the azapeptide drug through its

hydrogen bonds to the catalytic residues and to G48²⁵ was noticed.

Considering the most probable ATV configuration in the presence of the V82A mutation, a large number of nonbonded contacts and eight hydrogen bonds were identified. Nonetheless, such a substitution caused a less productive binding energy due to the loss of ATV interactions with the catalytic D29 (Figure 12B).

Finally, evaluating ATV recognition in the presence of the L76V mutation, numerous nonbonded contacts and nine hydrogen bonds were detected (Figure 12C). In particular, ATV showed hydrogen bonds to catalytic residues and to D29 of both chains, found to be crucial in substrate binding.²⁵ Such a profile is related to an increased drug affinity.

As reported in the literature, the PR dimer is maintained by interactions between the two subunits, including the terminal residues (1–4 and 96–99), the tips of the flaps (50, 51), D29, R8, and R8', and aminoacids in and surrounding the active site (residues 24–27).²⁵ Thus, in addition to the evaluation of the energetic and molecular recognition terms, the effects of the studied mutations were investigated in the context of the dimerization interface (Table 4).

In LPV complexes, in the presence of I84V mutation, a lower number of productive contacts at PR dimer interface was found. Conversely, the substitution L76V was associated

Table 4. List of LPV, APV, SQV, and ATV Interactions at the PR Dimerization Interface^{a,b}

res ^c	LPV			APV			SQV			ATV		
	WT	I84V	L76V	WT	M46I	L76V	WT	I84V	M46I	WT	V82A	L76V
P1	<i>a</i> * <i>b</i>	<i>a</i> * <i>b</i>	<i>a</i> * <i>b</i>	* <i>ab</i>	<i>a</i> * <i>b</i>	<i>a</i> * <i>b</i>	<i>a</i> * <i>b</i>	<i>a</i> * <i>b</i>	/	<i>a</i> * <i>b</i>	<i>a</i> * <i>b</i>	<i>a</i> * <i>b</i>
Q2	<i>ab</i>	<i>ab</i> *	<i>a</i> * <i>b</i>	/	<i>a</i> * <i>b</i>	<i>a</i> * <i>b</i>	* <i>ab</i>	<i>ab</i> *	<i>a</i> * <i>b</i>	<i>a</i> * <i>b</i>	<i>a</i> * <i>b</i>	<i>a</i> * <i>b</i>
I3	<i>a</i> * <i>b</i>	<i>a</i> * <i>b</i>	<i>a</i> * <i>b</i>	* <i>ab</i>	<i>a</i> * <i>b</i>	<i>a</i> * <i>b</i>	* <i>ab</i>	<i>a</i> * <i>b</i>				
T4	<i>ab</i>	<i>ab</i>	<i>ab</i>	<i>ab</i> *	<i>a</i>	<i>a</i>	<i>ab</i> *	<i>b</i>	<i>ab</i>	<i>ab</i>	<i>ab</i>	* <i>ab</i>
L5	<i>ab</i> *	<i>ab</i> *	<i>a</i> * <i>b</i>	<i>a</i> * <i>b</i>	* <i>ab</i>	* <i>ab</i>	<i>a</i> * <i>b</i>					
W6	<i>ab</i>	<i>ab</i>	<i>ab</i> *	<i>a</i> * <i>b</i>	<i>a</i> * <i>b</i>	* <i>ab</i>	<i>a</i> * <i>b</i>	<i>a</i> * <i>b</i>	* <i>ab</i>	* <i>ab</i>	<i>ab</i> *	<i>ab</i> *
Q7	<i>b</i> *	<i>ab</i> *	<i>b</i> *	<i>a</i> * <i>b</i>	* <i>ab</i>	* <i>ab</i>	<i>ab</i>	<i>a</i> *	<i>ab</i>	<i>a</i> * <i>b</i>	<i>a</i> * <i>b</i>	<i>ab</i>
R8	<i>a</i> * <i>b</i>	<i>a</i> * <i>b</i>	<i>a</i> * <i>b</i>	<i>b</i> *	<i>a</i> * <i>b</i>							
P9	<i>a</i>	<i>ab</i>	<i>ab</i>	<i>a</i>	<i>ab</i>							
V11	/	/	/	<i>a</i>	/	<i>a</i>	<i>b</i>	<i>b</i>	/	/	/	<i>a</i>
L23	/	/	<i>b</i>	/	<i>a</i>	<i>b</i>	/	/	/	/	/	/
L24	* <i>ab</i>	* <i>ab</i>	* <i>ab</i>	* <i>ab</i>	<i>ab</i> *	<i>ab</i>	<i>a</i>	<i>ab</i>	<i>ab</i>	<i>ab</i> *	<i>a</i>	<i>ab</i>
D25	<i>b</i> *	<i>b</i> *	<i>ab</i> *	<i>ab</i> *	<i>a</i>	<i>a</i> *	<i>ab</i> *	<i>ab</i> *	<i>ab</i> *	<i>a</i> *	<i>ab</i> *	<i>a</i> *
T26	<i>a</i> * <i>b</i>											
G27	<i>a</i> *	<i>a</i> * <i>b</i>	* <i>ab</i>	* <i>ab</i>	<i>b</i>	<i>ab</i> *	* <i>ab</i>	<i>a</i> * <i>b</i>	<i>b</i>	<i>b</i> *	* <i>ab</i>	<i>a</i> *
D29	<i>a</i> * <i>b</i>	<i>a</i> * <i>b</i>	<i>a</i> * <i>b</i>	<i>a</i> * <i>b</i>	<i>a</i> *	<i>a</i> * <i>b</i>						
V32	/	/	/	/	/	/	<i>b</i>	/	<i>b</i>	/	<i>a</i>	/
I47	<i>ab</i>	<i>a</i>	<i>ab</i>	<i>b</i>	<i>ab</i>	<i>ab</i>	<i>b</i>	<i>b</i>	<i>b</i>	<i>ab</i>	/	/
G48	<i>ab</i>	<i>a</i> * <i>b</i>	<i>b</i>	<i>ab</i>								
G49	* <i>ab</i>	<i>b</i>	<i>a</i>	<i>ab</i>	/	* <i>ab</i>	<i>ab</i>	<i>a</i>	<i>a</i>	<i>ab</i>	<i>b</i>	/
I50	<i>a</i> * <i>b</i>	<i>a</i> * <i>b</i>	<i>a</i> * <i>b</i>	<i>ab</i>	<i>ab</i>	<i>ab</i>	<i>ab</i>	<i>ab</i>	<i>ab</i> *	<i>a</i> * <i>b</i>	<i>a</i> * <i>b</i>	<i>ab</i> *
G51	<i>ab</i>	<i>a</i> * <i>b</i>	<i>ab</i> *	* <i>ab</i>								
G52	<i>ab</i> *	<i>ab</i>	<i>ab</i>	<i>ab</i>	<i>a</i>	<i>a</i>	<i>ab</i>	<i>ab</i>	* <i>ab</i>	<i>ab</i>	<i>b</i>	* <i>ab</i>
F53	<i>ab</i>	<i>ab</i>	/	<i>b</i>	<i>b</i>	/	<i>ab</i>	<i>ab</i>	<i>ab</i>	<i>a</i> *	<i>b</i>	<i>a</i>
I54	<i>b</i>	/	<i>ab</i>	<i>ab</i>	<i>ab</i>	<i>b</i>	<i>ab</i>	<i>ab</i>	<i>b</i>	<i>ab</i>	<i>ab</i>	<i>a</i>
I66	/	/	/	<i>a</i>	/	/	/	<i>a</i>	/	<i>b</i>	/	<i>a</i>
C67	/	/	<i>ab</i>	<i>a</i>	<i>b</i>	<i>ab</i>	<i>ab</i>	<i>ab</i>	<i>b</i>	<i>ab</i>	<i>a</i>	<i>ab</i>
H69	/	<i>ab</i>	<i>ab</i>	<i>a</i>	<i>ab</i>	<i>b</i>	<i>a</i>	<i>ab</i>	<i>ab</i>	<i>ab</i>	<i>b</i>	<i>a</i> *
P79	/	/	/	/	<i>a</i>	/	/	/	/	/	<i>a</i> *	/
T80	<i>b</i> *	/	<i>a</i>	<i>ab</i>	<i>a</i>	/	/	/	<i>b</i>	<i>a</i>	<i>a</i>	/
P81	/	/	/	<i>a</i>	/	/	<i>ab</i>	<i>b</i>	<i>ab</i>	/	<i>a</i>	/
I84	/	/	/	/	/	/	<i>b</i>	<i>b</i>	<i>b</i>	<i>b</i>	<i>a</i>	/
R87	<i>a</i> * <i>b</i>	<i>ab</i> *	* <i>ab</i>	<i>a</i> * <i>b</i>								
N88	<i>ab</i>	<i>a</i>	<i>ab</i>	<i>b</i>	/	<i>a</i>	/	/	/	<i>ab</i>	<i>b</i>	/
L90	/	/	/	<i>ab</i>	<i>a</i>	<i>ab</i>	<i>ab</i> *	<i>b</i> *	<i>a</i>	<i>a</i>	* <i>ab</i>	<i>a</i> *
T91	<i>ab</i>	<i>ab</i>	<i>ab</i>	* <i>ab</i>	<i>ab</i> *	<i>ab</i> *	<i>ab</i>	<i>ab</i>	<i>ab</i>	<i>ab</i>	<i>ab</i>	<i>ab</i>
Q92	<i>b</i>	<i>a</i>	<i>ab</i>	<i>b</i>	<i>b</i>	<i>a</i>	/	/	/	<i>ab</i>	<i>b</i>	/
I93	/	<i>b</i>	/	<i>ab</i>	<i>b</i>	<i>b</i>	/	<i>ab</i> *	<i>b</i>	<i>b</i>	/	<i>b</i>
G94	<i>ab</i>											
C95	* <i>ab</i>	<i>ab</i>	<i>ab</i>	* <i>ab</i>	<i>ab</i>	* <i>ab</i>	<i>a</i> * <i>b</i>	<i>a</i> * <i>b</i>	* <i>ab</i>	<i>ab</i>	* <i>ab</i>	<i>a</i> * <i>b</i>
T96	<i>a</i> * <i>b</i>											
L97	<i>a</i> * <i>b</i>											
N98	<i>a</i> * <i>b</i>											
F99	<i>a</i> * <i>b</i>											
no. of contacts	152	140	165	170	160	160	152	152	146	171	173	133

^a *a* and *b* indicate, respectively, the PR subunits pertinent to the specified residues establishing non-bonded contacts. ^b The asterisks point out hydrogen bonds. ^c The residue is reported as in the WT sequence.

with an increased network of interactions with respect to the WT sequence.

Analyzing the contacts at PR dimer region in APV complexes, both the selected mutations were related to a reduced protein stability.

In SQV complexes, WT and I84V structures reported a similar profile at the interface area, while in the presence of the M46I mutation a reduced number of interactions was observed.

Examining ATV complexes, V82A mutated enzyme was associated with a dimer stability comparable to WT, while in the presence of the L76V substitution a decreased network of interface contacts was found.

In order to evaluate the impact of the analyzed mutations onto the enzyme conformational changes, we started to take into account the active site flexibility. The catalytic triad (D25, T26, G27) of both subunits was considered to monitor

this effect. The root-mean-square deviation (RMSd) computed onto the Cα atoms of the catalytic triads during the MD trajectories revealed in all cases fluctuations lower than 0.8 Å. This observation is in agreement with published data, attesting a general conservation of the active site geometry in the presence of different drugs and mutations.^{14,16,21,28–31}

Then we continued our geometrical analysis with the flap region. It is well-known that the curling of the tips of this area triggers the opening of the entire flaps. In Perryman's work, the authors investigated the distribution of the "TriCa angle" (formed by three Cα atoms of the adjacent residues G48, G49, and I50) and observed, in the presence of mutations, such an angle with a broader distribution compared to WT.³² Since the "TriCa angle" seemed to be a widely accepted descriptor to evaluate the flexibility of the flap region, we monitored it in WT and mutated enzyme-complexes. As reported in Figure 13, for [LPV•PR],

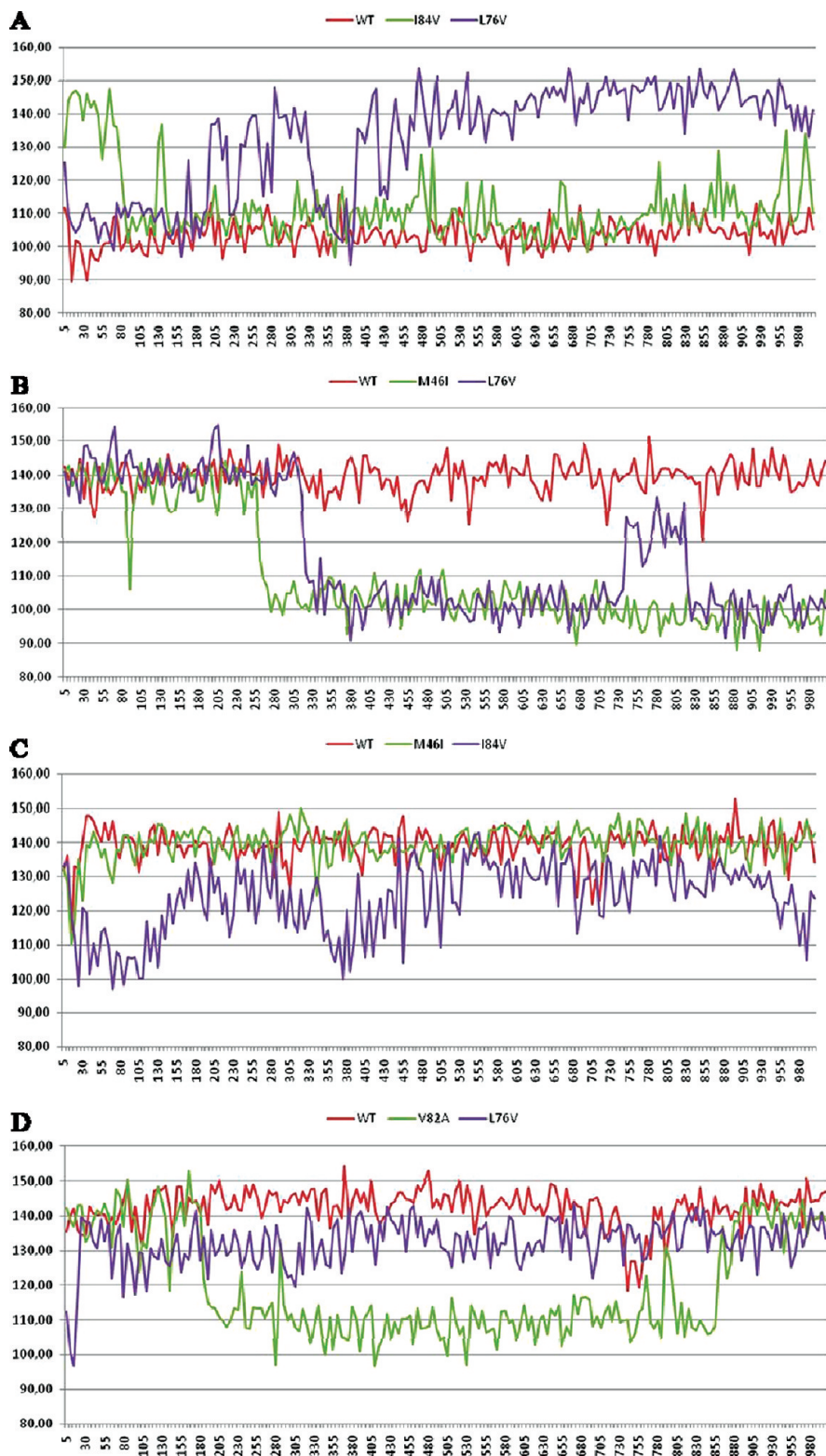


Figure 13. “TriCa angle”³² monitoring of (A) LPV, (B) APV, (C) SQV, and (D) ATV wild-type (red line) and mutated complexes (violet and green lines). On the abscissa axis is reported the simulation Time, expressed in ps, of the MD run, on the ordinate the value of the “TriCa angle”.

[APV·PR], and [SQV·PR] complexes, in the presence of the resistance-inducing mutations, a wider “TriCa angle” distribution was observed with respect to the WT sequence. The higher conformational flexibility of the flap region can explain the resistance data of mutated PR sequences. Interestingly, in [ATV·PR] complexes, the same observation can be found in the V82A mutant with large conformational

fluctuations, but in the L76V TriCa profile the angle is similar to the WT according to the hypersusceptibility data (Z-score equal to -0.30).

CONCLUSIONS

In conclusion we have developed and applied a computational protocol to selected combinations of PR sequences

and four approved PIs with the aim to link structural and thermodynamics data with relevant clinical results. The resistance, expressed as Z-score index, was related geometrically to the “TriCa angle” during the MD simulations and thermodynamically to free interaction energies in the fully optimized ensembles. By this approach the medicinal chemist can get additional information useful in the rational design of novel PIs active against to resistant PR mutants. The encouraging results obtained in our preliminary set of twelve combinations will push us to extend our analysis to a larger amount of PR-PI complexes and eventually to apply this computational strategy to other enzymatic targets subjected to resistance-inducing mutations. This work is currently in progress in our laboratory and will be the object of future communications.

EXPERIMENTAL SECTION

Clinical Section. For this study, we have analyzed 3248 pol sequences from 1802 HIV-1 B subtype patients naïve for antiretroviral drugs and from 1446 HIV-1 B subtype patients failing an antiretroviral regimen containing at least one PI, followed in different clinical departments in central Italy. Data for all patients were stored in a specifically designed anonymous database that included genotypic, demographic, immunologic, virologic, and therapeutic parameters.

HIV Sequencing. HIV-genotype analysis was performed on plasma samples by means of a commercially available kit (The ViroSeq HIV-1 Genotyping System, AB). Briefly, RNA was extracted, retrotranscribed by MULV RT, and amplified with ampliTaq-Gold polymerase enzyme by using 2 different sequence-specific primers for 40 cycles. Pol amplified products (containing the entire protease and the first 320 amino acids of the reverse transcriptase open reading frame) were full-length sequenced in sense and antisense orientations by using 7 different overlapping sequence-specific primers by an automated sequencer (ABI 3100). Sequences having a mixture of wild-type and mutant residues at single positions were considered to have the mutation(s) at that position. The isolates were subtyped by comparing them to reference sequences of known subtype.³³

COMPUTATIONAL SECTION

Association with Phenotypic NNRTI Susceptibility. We measured the impact of L76V, V82A, I84V, and M46I on PI resistance in multivariate computational models for predicting phenotypic resistance from genotype. In contrast to the univariate setting, multivariate analyses allow for assessing the impact of mutations relative to other mutations. Specifically, we analyzed the support vector regression models used in the *geno2pheno* Web-based prediction service,³⁴ by exploiting the bilinearity of the kernel used in *geno2pheno*, according to the method described by Sing et al.¹³ These models are based on approximately 850 matched genotype-phenotype pairs derived from another recombinant assay and are part of the German Arevir database.

Structural Analysis. For all PR inhibitors the analyzed mutant models were built, starting from crystallographic data, by replacing residues. Theoretical structures were energy minimized using the united atom AMBER* force field³⁵ and the GB/SA water implicit solvation model.³⁶ Using the same

force field and environment, the optimized models were submitted to 1 ns of MD simulation at 300 K, with a time-step equal to 1.0 fs, sampling 200 structures at regular time intervals.

Starting from the most probable MD geometry, all the analyzed complexes were submitted to Monte Carlo *in situ* simulations using the same force field and solvation conditions of MD run. 100 conformations were randomly generated allowing the free rotation of PIs rotatable bonds, energy minimized with 2000 iterations of the PRCG method, up to 0.5 kJ/Å·mol convergence. The *in situ* MC simulations were carried out adding a MOLS keyword for each drug into the command directive file, fixing a ligand atom corresponding to the center of the PI. After checking the convergence in the MC generation, all the obtained structures were optimized by 2000 iterations of full energy minimization with a convergence RMSd equal to 0.125 Å.

These calculations were performed with the molecular modeling software MacroModel ver. 7.2.³⁷

According to the Moline method,³⁸ the interaction energies of all PR complexes were evaluated, in the ensemble of all optimized configurations. The ligand-enzyme and PR dimer interface contacts were analyzed by the LigPlot program³⁹ using the most probable optimized configurations.

ACKNOWLEDGMENT

This work was supported by the project AMICO of the INFN.

REFERENCES AND NOTES

- Wlodawer, A. Rational approach to AIDS drug design through structural biology. *Annu. Rev. Med.* **2002**, *53*, 595–614.
- Miller, M.; Jaskolski, M.; Rao, J. K. M.; Leis, J.; Wlodawer, A. Crystal structure of a retroviral protease proves relationship to aspartic protease family. *Nature* **1989**, *337*, 576–579.
- Rao, J. K. M.; Erickson, J. W.; Wlodawer, A. Structural and evolutionary relationships between retroviral and eukaryotic aspartic proteinases. *Biochemistry* **1991**, *30*, 4663–4671.
- Davies, D. R. The structure and function of the aspartic proteinases. *Annu. Rev. Biophys. Biophys. Chem.* **1990**, *19*, 189–215.
- Protein Data Bank. <http://www.rcsb.org/PDB> (accessed February 2009).
- Tomasselli, A. G.; Howe, W. J.; Sawyer, T. K.; Wlodawer, A.; Heinrikson, R. L. The complexities of AIDS: an assessment of the HIV protease as a therapeutic target. *Chim. Oggi* **1991**, *9*, 6–27.
- Wlodawer, A.; Erickson, J. W. Structure-based inhibitors of HIV-1 protease. *Annu. Rev. Biochem.* **1993**, *62*, 543–585.
- Svicher, V.; Ceccherini-Silberstein, F.; Erba, F.; Santoro, M.; Gori, C.; Bellocchi, M. C.; Giannella, S.; Trotta, M. P.; Monforte, A.; Antinori, A.; Perno, C. F. Novel human immunodeficiency virus type 1 protease mutations potentially involved in resistance to protease inhibitors. *Antimicrob. Agents Chemother.* **2005**, *49*, 2015–2025.
- Hertogs, K.; Van Houtte, M.; Larder, B. A. Testing for HIV-1 drug resistance: new development and clinical implications. *Recent Res. Dev. Antimicrob. Agents Chemother.* **1999**, *3*, 83–104.
- Johnson, V. A.; Brun-Vezinet, F.; Clotet, B.; Conway, B.; D'Aquila, R. T.; Demeter, L. M.; Kuritzkes, D. R.; Pillay, D.; Schapiro, J. M.; Telenti, A.; Richman, D. D. Update of the drug resistance mutations in HIV-1: 2004. *Top. HIV Med.* **2004**, *12*, 119–124.
- Hirsch, M. S.; Günthard, H. F.; Schapiro, J. M.; Brun-Vézinet, F.; Clotet, B.; Hammer, S. M.; Johnson, V. A.; Kuritzkes, D. R.; Mellors, J. W.; Pillay, D.; Yeni, P. G.; Jacobsen, D. M.; Richman, D. D. Antiretroviral drug resistance testing in adult HIV-1 infection: 2008 recommendations of an International AIDS Society-USA panel. *Clin. Infect. Dis.* **2008**, *47*, 266–285.
- Poveda, E.; de Mendoza, C.; Parkin, N.; Choe, S.; García-Gasco, P.; Corral, A.; Soriano, V. Evidence for different susceptibility to tipranavir and darunavir in patients infected with distinct HIV-1 subtypes. *AIDS* **2008**, *22*, 611–616.
- Beerenwinkel, N.; Sing, T.; Lengauer, T.; Rahnenführer, J.; Roomp, K.; Savenkov, I.; Fischer, R.; Hoffmann, D.; Selbig, J.; Korn, K.;

- Walter, H.; Berg, T.; Braun, P.; Fätkenheuer, G.; Oette, M.; Rockstroh, J.; Kupfer, B.; Kaiser, R.; Däumer, M. Computational methods for the design of effective therapies against drug resistant HIV strains. *Bioinformatics* **2005**, *21*, 3943–3950.
- (14) Hou, T.; Yu, R. Molecular Dynamics and Free Energy Studies on the Wild-type and Double Mutant HIV-1 Protease Complexed with Amprenavir and Two Amprenavir-Related Inhibitors: Mechanism for Binding and Drug Resistance. *J. Med. Chem.* **2007**, *50*, 1177–1188.
- (15) Paulsen, D.; Elston, R.; Snowden, W.; Tisdale, M.; Ross, L. Differentiation of genotypic resistance profiles for amprenavir and lopinavir, a valuable aid for choice of therapy in protease inhibitor-experienced HIV-1-infected subjects. *J. Antimicrob. Chemother.* **2003**, *52*, 319–323.
- (16) Liu, F.; Kovalevsky, A. Y.; Tie, Y.; Ghosh, A. K.; Harrison, R. W.; Weber, I. T. Effect of Flap Mutations on Structure of HIV-1 Protease and Inhibition by Saquinavir and Darunavir. *J. Mol. Biol.* **2008**, *381*, 102–115.
- (17) Roberts, N. A. Drug-resistance patterns of saquinavir and other HIV protease inhibitors. *AIDS* **1995**, *9* (Suppl. 2), 27–S32.
- (18) Weinheimer, S.; Discotto, L.; Friberg, J.; Yang, H.; Colombo, R. Atazanavir signature I50L resistance substitution accounts for unique phenotype of increased susceptibility to other protease inhibitors in a variety of human immunodeficiency virus type 1 genetic backbones. *Antimicrob. Agents Chemother.* **2005**, *49*, 3816–3824.
- (19) Stoll, V.; Qin, W.; Stewart, K. D.; Jakob, C.; Park, C.; Walter, K.; Simmer, R. L.; Helfrich, R.; Bussiere, D.; Kao, J.; Kempf, D.; Sham, H. L.; Norbeck, D. W. X-ray crystallographic structure of ABT-378 (lopinavir) bound to HIV-1 protease. *Bioorg. Med. Chem.* **2002**, *10*, 2803–2806.
- (20) Surleraux, D. L. N. G.; Tahri, A.; Verschueren, W. G.; Pille, G. M. E.; de Kock, H. A.; Jonckers, T. H. M.; Peeters, A.; De Meyer, S.; Azijn, H.; Pauwels, R.; de Bethune, M. P.; King, N. M.; Prabu-Jeyabalan, M.; Schiffer, C. A.; Wigerinck, P. B. T. P. Discovery and selection of TMC114, a next generation HIV-1 protease inhibitor. *J. Med. Chem.* **2005**, *48*, 1813–1822.
- (21) Tie, Y.; Kovalevsky, A. Y.; Boross, P.; Wang, Y. F.; Ghosh, A. K.; Tozser, J.; Harrison, R. W.; Weber, I. T. Atomic resolution crystal structures of HIV-1 protease and mutants V82A and I84V with saquinavir. *Proteins* **2007**, *67*, 232–242.
- (22) Armstrong, A. A.; Muzammil, S.; Jakalian, A.; Bonneau, P. R.; Schmelmer, V.; Freire, E.; Amzel, L. M. Unique Thermodynamic Response of Tipranavir to Human Immunodeficiency Virus Type 1 Protease Drug Resistance Mutations. *J. Virol.* **2007**, *81*, 5144–5154.
- (23) Lyne, P. D.; Lamb, M. L.; Saeh, J. C. Accurate Prediction of the Relative Potencies of Members of a Series of Kinase Inhibitors Using Molecular Docking and MM-GBSA Scoring. *J. Med. Chem.* **2006**, *49*, 4805–4808.
- (24) Weber, I. T.; Cavanaugh, D. S.; Harrison, R. W. Models of HIV-1 protease with peptides representing its natural substrates. *J. Mol. Struct.* **1998**, *423*, 1–12.
- (25) Sayer, J. M.; Liu, F.; Ishima, R.; Weber, I. T.; Louis, J. M. Effect of the active-site D25N mutation on the structure, stability and ligand binding of the mature HIV-1 protease. *J. Biol. Chem.* **2008**, *283*, 13459–13470.
- (26) Shafer, R. W.; Rhee, S. Y.; Pillay, D.; Miller, V.; Sandstrom, P.; Schapiro, J. M.; Kuritzkes, D. R.; Bennett, D. HIV-1 protease and reverse transcriptase mutations for drug resistance surveillance. *AIDS* **2007**, *21*, 215–223.
- (27) Sadiq, S. K.; Wan, S.; Coveney, P. V. Insights into a Mutation-Assisted Lateral Drug Escape Mechanism from the HIV-1 Protease Active Site. *Biochemistry* **2007**, *46*, 14865–14877.
- (28) Liu, F.; Kovalevsky, A. Y.; Louis, J. M.; Boross, P. I.; Wang, Y. F.; Harrison, R. W.; Weber, I. T. Mechanism of drug resistance revealed by the crystal structure of the unliganded HIV-1 protease with F53L mutation. *J. Mol. Biol.* **2006**, *358*, 1191–1199.
- (29) Kovalevsky, A. Y.; Liu, F.; Leshchenko, S.; Ghosh, A. K.; Louis, J. M.; Harrison, R. W.; Weber, I. T. Ultrahigh resolution crystal structure of HIV-1 protease mutant reveals two binding sites for clinical inhibitor TMC114. *J. Mol. Biol.* **2006**, *363*, 161–173.
- (30) Liu, F.; Boross, P. I.; Wang, Y. F.; Tozser, J.; Louis, J. M.; Harrison, R. W.; Weber, I. T. Kinetic, stability, and structural changes in high-resolution crystal structures of HIV-1 protease with drug-resistant mutations L24I, I50V, and G73S. *J. Mol. Biol.* **2005**, *354*, 789–800.
- (31) Zoete, V.; Michielin, O.; Karplus, M. Relation between sequence and structure of HIV-1 protease inhibitor complexes: a model system for the analysis of protein flexibility. *J. Mol. Biol.* **2002**, *315*, 21–52.
- (32) Perryman, A. L.; Lin, J. H.; McCammon, J. A. HIV-1 protease molecular dynamics of a wild-type and of the V82F/I84V mutant: Possible contributions to drug resistance and a potential new target site for drugs. *Protein Sci.* **2004**, *13*, 1108–1123.
- (33) Stanford Database. <http://hivdb.Stanford.edu> (accessed February 2009).
- (34) geno2pheno Web-based prediction service. <http://www.geno2pheno.org> (accessed February 2009).
- (35) McDonald, D. Q.; Still, W. C. AMBER torsional parameters for the peptide backbone. *Tetrahedron Lett.* **1992**, *33*, 7743–7746.
- (36) Still, W. C.; Tempczyk, A.; Hawley, R. C.; Hendrickson, T. Semi-analytical treatment of solvation for molecular mechanism and dynamics. *J. Am. Chem. Soc.* **1990**, *112*, 6127–6129.
- (37) Mohamadi, F.; Richards, N. G. J.; Guida, W. C. MacroModel: an integrated software system for modeling organic and bioorganic molecules using molecular mechanics. *J. Comput. Chem.* **1990**, *11*, 440–467.
- (38) Alcaro, S.; Gasparini, F.; Incani, O.; Muccetti, S.; Misiti, D.; Pierini, M.; Villani, C. A “quasi-flexible” automatic docking processing for studying stereoselective recognition mechanisms. Part I. Protocol validation. *J. Comput. Chem.* **2000**, *21*, 515–530.
- (39) Wallace, A. C.; Laskowski, R. A.; Thornton, J. LIGPLOT: a program to generate schematic diagrams of protein-ligand interactions. *Protein Eng.* **1995**, *8*, 127–134.

CI900012K